

NSF GRANT # DMI - 0500453
 NSF PRORAM NAME: Materials Processing & Manufacturing

GOALI:

Online Dynamic Control of Cooling in Continuous Casting of Thin Steel Slabs

B.G. Thomas (PI)

University of Illinois at Urbana-Champaign
 Department of Mechanical Science and Engineering
 1206 West Green Street, Urbana, IL 61801
 Email: bgthomas@uiuc.edu

J. Bentsman (co-PI), B. Petrus, X. Zhou, K. Zheng, S. Vapalahti, H. Li

University of Illinois, Urbana, Illinois

A.H. Castillejos and F.A. Acosta
 Cinvestav, Saltillo, Mexico

Abstract: A model-based system has been developed to control secondary cooling of continuous casting machines in commercial steel plants, in order to maintain desired temperature setpoints in real time. This is important to optimize the quality of continuous-cast semi-finished steel shapes, which are used for 96% of the 100 million tons of steel produced in the U.S. each year.

The system features a fast, accurate transient computer model of heat transfer during the solidification process that serves as a “software sensor”, to provide feedback to a control system. Operating conditions are input from the level 2 automation system and the spray-water flow rates in the secondary cooling zone of the caster are continuously adjusted, in order to maintain the desired temperature profile throughout the steel. The system is being calibrated, using thermocouple and optical temperature sensors, tested and implemented at an operating U.S. thin slab caster.

This multifaceted project has achieved significant results on several different subprojects. The transient finite difference model, CONID, has been optimized to run in an online environment and serves as the software sensor. A new control system has been developed using

CONID and has been demonstrated to be capable of stable tracking of the setpoints in real time, using a robust control algorithm that features anti-windup. Testing has shown it outperforms the existing control system used at the steel plant. After rigorous testing, the system has been implemented into a commercial thin-slab caster, and tangible improvements have already been realized. An ambitious experimental program to measure spray cooling coefficients is also underway, including a novel induction-heating system that is capable of measuring heat transfer rates at constant surface temperature. Pyrometer measurements have been made at the steel plant to validate the temperature predictions. Finally, related work is proceeding on controlling fluid flow in the mold and in understanding of defect formation, in order to facilitate setpoint generation, so that cracks and other defects can be minimized.

Future improvements to this novel model-based control system could revolutionize the control of continuous casting spray systems, with improved steel quality, and will have beneficial impact on related scientific fields and commercial processes.

1. Introduction: For the high-volume low-profit-margin steel industry to compete in the world market, it must improve efficiency and consistency of steel quality. Implementing better control systems for the continuous casting process is one way to achieve this. Continuous casting produces 96% of steel in the U.S. and the fraction of the new high-speed thin-slab casting process is growing every year.^[1] Temperature variations during cooling in this process cause quality problems such as cracks, especially under transient conditions.^[2] Thus, there is great incentive to implement control systems to optimize spray cooling to maintain the desired optimal temperature profiles.

Secondary cooling presents control challenges. Conventional feedback control systems cannot, however, be used for this purpose due to the insufficient reliability of temperature sensors. Thin-slab casting is particularly difficult because the high casting speed requires faster response. Modern air-mist cooling nozzles offer the potential advantages of faster and more uniform cooling, but introduce the extra challenge of air flow rate as another process variable to control. Recent model-based predictive control systems face special problems in thin slab casting, owing to the higher speed and the increased relative importance of solidification in the mold, which is not easy to predict accurately.

Previous studies, including those of the principal investigators, have developed comprehensive computational models of the continuous casting process based on nonlinear parabolic partial differential equations (PDEs). The accuracy of these models to predict heat transfer and solidification has been demonstrated through comparison with analytical solutions and plant measurements. This work has led to improved fundamental insights into the process.

The objective of this work is 1) to develop a fast and accurate thermal model of thin slab casting and 2) to implement this model into a fundamentally-based system to dynamically control the spray flow rates for cooling optimization of this process.

To achieve this goal requires i) efficient numerical algorithms to synthesize the first online temperature “software sensor” calibrated in real time through reliable online measurements; ii) lab measurements of spray-water cooling to improve the accuracy of model predictions through better characterization of the boundary conditions; iii) one-time plant measurements obtained at the caster specifically instrumented for this purpose, iv) better control design tools, applicable to this class of nonlinear parabolic PDEs, and v) the application of other tools to improve understanding of the process, so that better temperature setpoint profiles can be found to optimize spray cooling.

This effort combines the talents of a team of researchers, including the experience of B.G. Thomas in mathematical modeling of continuous casting, Prof. J. Bentsman in adaptive control theory of distributed parameter systems and predictive control, experienced student researchers to carry out the work, and an industry team, led by Dr. Ron O’Malley of Nucor Steel, Decatur, Alabama, which are helping to conduct the plant measurements needed for model calibration, and are overseeing the implementation of the UIUC control algorithms into the level-2 control system of their plant. In addition, H. Castillejos is leading experimental efforts to better understand heat transfer in the spray zones. This project enhances and complements the modeling efforts at the University of Illinois Continuous Casting Consortium, created in 1989 by Prof. Thomas and currently supported by nine member companies.

Along with fundamental scientific benefits, the research proposed will have broader impacts. The direct broad impact of the effort proposed is quality improvement, cost reduction, and energy saving in continuous casting of thin steel slabs. This impact is strongly amplified by the rapid growth of thin slab casting in the steel industry. In addition, improved understanding of the control issues and algorithms will broadly benefit other high-speed manufacturing processes as well. The research will educate students who will take the modeling and control tools and technologies developed into industry. Most of all, the significant improvement of this key manufacturing process will be of direct benefit to society at large.

2. The Process: A schematic of steel processing is depicted in **Fig. 1**, with a close-up of the region between two rolls in the spray zone given in **Fig. 2**.

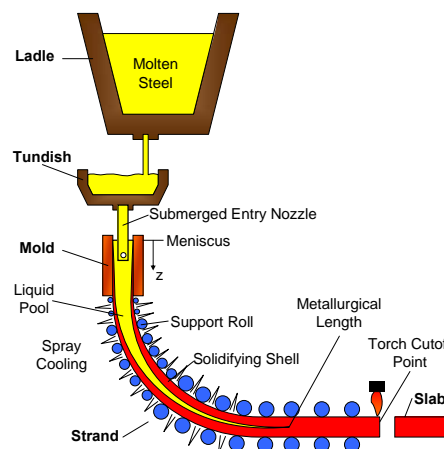


Fig. 1. Schematic of steel processing including ladle, tundish, and continuous casting

Steel flows from a ladle, through a “tundish,” and then exits down through a ceramic Submerged Entry Nozzle (SEN) into the mold. In the mold, the steel freezes against the water-cooled copper walls to form a thin solid shell, which is continuously withdrawn from the bottom of the mold at a “casting speed” that matches the flow rate of the incoming metal. The casting speed must be controlled to be slow enough to enable the shell to become sufficiently thick to support the liquid pool it contains, in order to avoid a catastrophic “breakout”, where molten steel penetrates the shell to drain over the bottom of the machine.

The steel strand then moves through the spray cooling zones, where water and air-mist sprays impact its surface to maintain cooling. Motor-driven drive rolls located below the mold continuously withdraw the strand downward. Many closely-spaced support rolls prevent the outward bulging of the shell due to the ferrostatic pressure arising from the liquid steel core. Water sprays emerge from high-pressure nozzles, which are interspaced between the support rolls and cool the strand during the solidification process. Other strategically placed rolls bend the shell to follow a curved path and then straighten it flat prior to torch cut-off into individual slabs. Start-up of this process is a relatively rare occurrence, and is achieved by inserting a “dummy” bar to plug the mold bottom.

The rolls support the wide surface to prevent bulging, but greatly affect the temperature distribution. As shown in **Fig. 2**, sharp drops in surface temperature are experienced beneath each roll, and beneath the impacting spray jet. Reheating occurs in the adjacent regions which are protected thermally by the space under the rolls. Gravity significantly affects the water boundary layer, which causes cooling to vary above and below the jet, and between the inside and outside surfaces of the strand. The water spray rates should be continuously adjusted to maintain a desired surface temperature profile to avoid the formation of surface cracks. Cracks are caused by thermal stress combined with metallurgical embrittlement due to nonmetallic precipitates and grain growth, which depend mainly on cooling history. Spray control is difficult, because sensors such as optical pyrometers are often unreliable due to intermittent steam and surface emissivity variations. Thus, they cannot be used for online feedback-control.

After exiting the spray cooling zones, the steel strand surface reheats, as natural convection and radiation heat extraction is small. The strand is no longer supported by rolls, so should be fully solidified. If any liquid core remains beyond the zone of roll support, the strand will bulge catastrophically, creating a thick “whale” shape, which forces costly shutdown of the process.

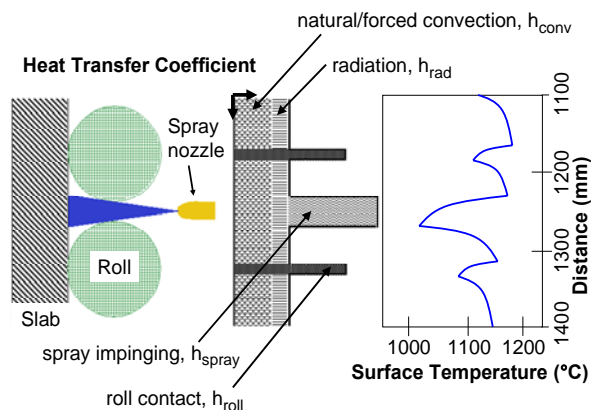


Fig. 2. Schematic of the spray region of the thin-slab steel caster, and corresponding heat transfer, and surface temperature profiles.

3. The Problem: The strand is subject to a variety of cracking problems during secondary spray cooling, such as transverse midface and corner cracks. These surface defects require expensive surface-reconditioning or even rejection of the product. These quality problems are generally caused by non-optimal cooling conditions, which arise due to unaccommodated variations in the process, such as changes in casting speed or mold powder cooling conditions. Most operations simply scale the water flow rate with casting speed. This does not provide uniform cooling, however. For example, after a temporary drop in casting speed, the colder strand near the top of the caster will need less water for a long time, while the strand near the bottom of the caster will be gone in a short time. As another example, a change in mold powder crystallization can drop the heat flux temporarily, causing a region of hotter, thinner shell at mold exit, which requires more cooling for the rest of its time in the caster. The strategy for controlling the water flow rates in spray zones should dynamically adjust for each portion of the strand, according to its entire history.

Traditional control strategies to maintain the strand surface temperature to a desired profile would utilize feedback based on temperature measurement at various places in the spray zones. However, the intermittent surface scale layer and harsh environment of the steamy spray chamber makes optical temperature sensors (pyrometers) unreliable. Thus, heuristic-based, open-loop control with a predictive model is the only successful control strategy to date. Model-based predictive control systems face special problems in thin slab casting, owing to the higher casting speed and the increased relative importance of solidification in the mold, which is not easy to predict accurately. Thin slab

casters are more prone to cracking problems than conventional casters, which prevents them from entering certain markets. Thus, there is great incentive to develop an improved model-based control system to optimize spray cooling, especially for the thin slab casting process.

4. Current Results: The results of this project are contained in 16 publications to date,^[3-18] a pending patent,^[19] and in our website <http://ccc.mechse.uiuc.edu>. This paper reports on seven different components of this multifaceted research project:

- 1) Efficient fundamental model of solidification and temperature in thin slab casting: CON1D
- 2) Software Sensor, CONONLINE
- 3) Online control system development and testing
- 4) Laboratory measurement of water flow and heat transfer during spray cooling
- 5) Steel plant experiments for model validation
- 6) Understanding defect formation during continuous casting
- 7) Control of mold fluid flow
- 8) Advance Control Algorithm Development

5. Efficient fundamental model of solidification and temperature in thin slab casting CON1D: The finite-difference model, CON1D, is a simple but comprehensive fundamentally-based model of heat transfer and solidification of the continuous casting of steel slabs, including phenomena in both the mold and the spray regions.^[20] The accuracy of this model in predicting heat transfer and solidification has been demonstrated through comparison with analytical solutions and plant measurements.^[20]

The simulation domain of CON1D, shown in **Fig. 3**, is a transverse slice through the strand thickness that spans from the center of shell surface of the inner radius to that of the outer radius. The CON1D model computes the temperature and solidification history of the slice as it traverses the path from the meniscus down through the spray zones to the end of the caster.

CON1D solves the 1-D transient heat conduction equation within the solidifying steel shell:

$$\rho_{steel} C p_{steel}^* \frac{\partial T}{\partial t} = k_{steel} \frac{\partial^2 T}{\partial x^2} + \frac{\partial k_{steel}}{\partial T} \left(\frac{\partial T}{\partial x} \right)^2 \quad [1]$$

This fundamentally-based model predicts shell thickness, temperature distribution, heat flux profiles down the mold face, metallurgical length, and other phenomena. The calculation takes advantage of the high Peclet number of the process, which renders axial heat conduction negligible. The heat flux profile in the

mold is based on the measured mold temperature rise and flow rate.

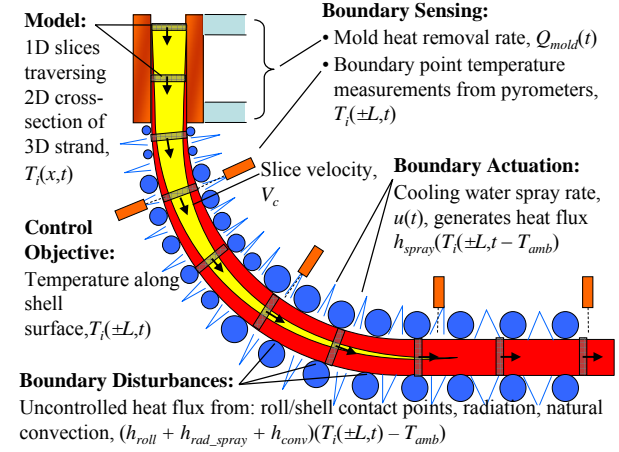


Fig. 3. CON1D simulation domain

Below the mold, heat flux from the strand surface varies greatly between each pair of support rolls according to spray nozzle cooling (based on water flux), h_{spray} ; radiation, h_{rad_spray} ; natural convection, h_{conv} ; and heat conduction to the rolls, h_{roll} , as shown in **Fig. 2**. Incorporating these phenomena enables the model to simulate heat transfer during the entire continuous casting process. The heat extraction due to water sprays is a function of water flow^[2] of the following form:

$$h_{spray} = A \cdot Q_{water}^c \cdot (1 - b \cdot T_{spray}) \quad [2]$$

where Q_{water} (l/m^2s) is water flux in spray zones and T_{spray} is the temperature of the spray cooling water. The constants in this empirical correlation are modified from Nozaki,^[21] which has been used successfully in previous models^[2, 22] Very recent experimental work is being undertaken as part of this project to measure these coefficients more accurately, including the effects of air mist cooling, and the enhanced heat transfer rates associated with intermittent boiling called the “Leidenfrost” effect.

Radiation is calculated by:

$$h_{rad_spray} = \sigma \cdot \epsilon_{steel} (T_{sK} + T_{ambK}) (T_{sK}^2 + T_{sprayK}^2) \quad [3]$$

where T_{sK} and T_{sprayK} are T_s and T_{spray} expressed in Kelvin. Natural convection is treated as a constant input for every spray zone. For water-cooling only, it is not very important, therefore it is simplified to $8.7W/m^2K$ everywhere. Larger values can be entered for h_{conv} to reflect the stronger convection when there is air mist in the cooling zone. Heat extraction into the rolls is calculated based on the fraction of heat extraction to the rolls, f_{roll} , which is calibrated for each spray zone. A typical f_{roll} value of 0.05 produces local temperature drops beneath the rolls of about $100^\circ C$. Beyond the

spray zones, heat transfer simplifies to radiation and natural convection. Further details on the model equations, boundary conditions, numerical discretization, previous validation efforts and other applications are given elsewhere.^[20]

An example of the predicted surface temperature history of the slice is given in **Fig. 4**. Notice that there are a number of temperature peaks and dips. The temperature dips are caused by water spray impingement and roll contact, whereas the temperature peaks occur where convection and radiation are the only mechanisms of heat extraction.

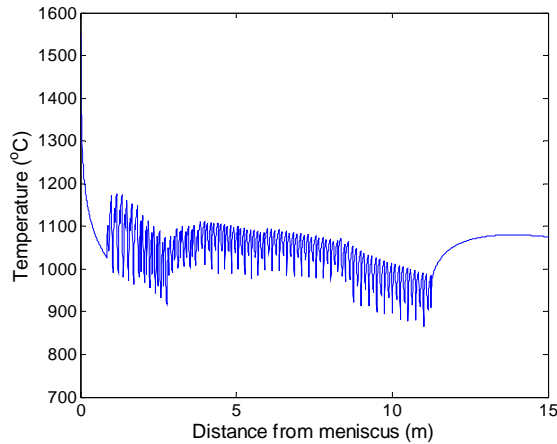


Fig. 4. Example of CON1D output: slice surface temperature history

The CON1D program has been optimized to run in less than 0.5s on a personal computer. This faster-than-real-time speed is necessary for it to become part of an online control system that updates every 1s.

In addition to successful model-based prediction and control capability, the model was used to generate setpoints for typical casting conditions. Specifically, 72 set points were generated for the Nucor caster to allow operation at 8 different spray-water patterns over a range of casting speeds (discretized as 9 different speeds over the maximum speed range). These set points are temperature profiles generated by CON1D using typical mold heat flux dependent on casting parameters which includes casting speed.^[23, 24]

The model is now ready to calibrate, validate, and implement as a software sensor into a control system.

6. Software Sensor CONSENSOR: The function of the software sensor is to accurately predict the temperature distribution in the strand in real time. The program CONSENSOR was developed to produce the

temperature profile along the entire caster (z) and through its thickness (x) in real time (t), by exploiting CON1D as a subroutine. It does this by managing the simulation of N different CON1D slices, each starting at the meniscus at a different time to achieve a fixed z -distance spacing between the slices. This is illustrated in **Fig. 5** using $N = 10$ slices for simplicity.

The control algorithm requires that CONSENSOR provide an updated surface temperature estimate, $\hat{T}(z, t)$, every Δt seconds. Note that the coordinates for T_i in CON1D slices (distance through thickness and time) are not the same as the coordinates for \hat{T} in CONSENSOR (distance from meniscus and time). The surface temperature estimate \hat{T} is assembled from the slice profile histories T_i , as follows.

During each time interval, the N different CON1D simulations track the evolution of temperature in each slice over this interval, given the previously-calculated and stored temperature distributions across the thickness of that slice at the start of the interval. The computation time required is about the same as just one complete CON1D simulation of the entire caster length, which takes about 0.6 seconds on the CentOS workstation when casting at 4.5 m/min.

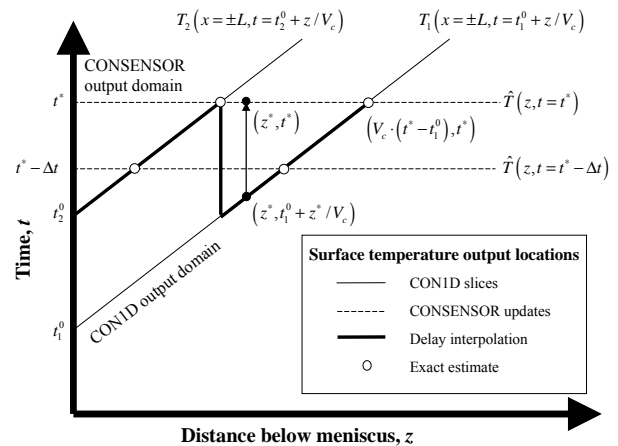


Fig. 5. Illustration of incremental runs of CON1D and shell surface temperature profile approximation using multiple slices with delay interpolation

During program startup, the simulation for slice $i + 1$ begins when slice i passes 75 mm from the meniscus. After startup, a new slice begins immediately from the meniscus whenever a slice reaches the end of the caster. Currently, CONSENSOR always manages exactly 200 slices, which corresponds to a uniform spatial interval of 75mm along the caster length, z_c , which is 15m. The complete temperature history for each slice is stored

from when it started at the meniscus, t_i^0 , to the current time, t . To assemble the complete temperature profile needed each time interval requires careful interpolation of the results of each slice at different times.

When plotted on a two-dimensional t - z grid, the desired output domain of the software sensor is a horizontal line, as shown in **Fig. 5**. For instance, at time t^* the sensor must predict $\hat{T}(z, t^*)$ for the entire caster length, $0 \leq z \leq z_c$. However, the surface temperature included in a single slice history from CON1D traverses a monotonic-increasing curve in the t - z plane. At constant casting speed, V_c , these curves are straight diagonal lines with slope of $1/V_c$. **Fig. 5** shows two such lines representing two slices created at times t_1^0 and t_2^0 .

It is clear from **Fig. 5** that each complete run of CON1D contributes only one data point to the desired software sensor output at each time, e.g. $\hat{T}(z_i(t^*), t^*)$, where $z_i(t)$ is the location of the i th slice at time t , which is calculated by

$$z_i(t) = \int_{t_i^0}^t V_c d\tau, \quad i = 1, 2, \dots, 200. \quad [4]$$

With constant casting speed, this integral simplifies to $V_c(t - t_i^0)$, (**Fig. 5**). Data points in the temperature profile estimate such as $\hat{T}(z_i(t^*), t^*)$, which come directly from CON1D output, are exact estimation points.

Fig. 6 illustrates the error introduced by interpolating spatially between these exact points. The 75 mm span between slices in this work can pass over the temperature dips and peaks caused by the roll and spray spacing, resulting in errors of 100 °C or more. This problem is overcome by “delay interpolation,” interpolating temporally between the latest temperature histories available from each CON1D slice, described as follows and illustrated in **Fig. 6** using $N = 2$ slices.

For locations between the exact estimate points, the surface temperature is approximated at the current time using the most recent available temperature at that location from the CON1D slice histories. Applying this method everywhere along the caster, the control-oriented shell surface temperature profile prediction $\hat{T}(z, t)$ is obtained at any time t :

$$\hat{T}(z, t) = T_i(x = \pm L, t = t_i(z)), \quad [5]$$

where $z_{i+1}(t) < z \leq z_i(t)$

where $z_i(t)$ is given in Eq. 4, and $t_i(z)$ is the time when the i^{th} slice was the distance z from the meniscus, which is the inverse of Eq. 4:

$$t_i(z) = t_i^0 + \int_0^z \frac{d\zeta}{V_c} \quad [6]$$

For constant casting speed, this simplifies to $t_i^0 + z/V_c$.

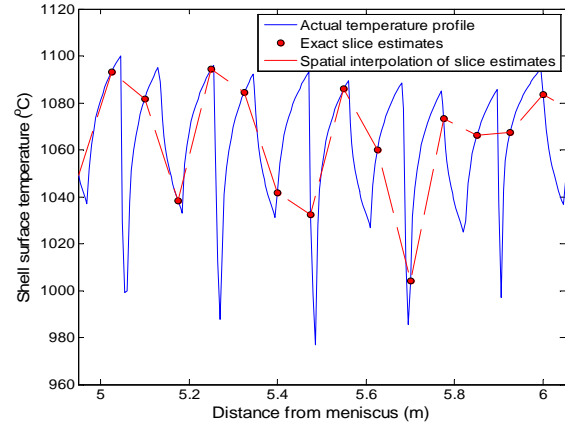


Fig. 6. Example of the actual temperature profile, the exact estimates and spatially interpolated temperature profile

Fig. 5 illustrates this process at time t^* . Starting from the previous time, $t^* - \Delta t$, the simulation restarts for each slice and continues for the desired time interval, Δt , giving temporally-exact estimates at two new locations at time t^* . The point (z^*, t^*) lies in between the locations of these exact estimates, so according to the delay interpolation scheme, the surface temperature at this point is approximated by the surface temperature of slice 1 when it passed the distance z^* from the meniscus. Thus, the temperature $T_1(\pm L, t_1^0 + z^*/V_c)$ from the history of slice 1 is used to estimate the surface temperature $\hat{T}(z^*, t^*)$.

The approximation error introduced at location z^* in **Fig. 5** is the temperature change at this location from time $t_1(z^*)$ to $t^* + \Delta t$, which is a function of the extent of transient effects in the laboratory frame, and slice spacing. It follows that slices should be evenly distributed to minimize the approximation error, and that the magnitude of this error decays to zero during steady operation. Even during times of extreme

transients, this error is easily recognized by operators from the jagged appearance of the temperature profile, as it jumps from locations with the worst delays to the exact points. Note that the interpolation delay for the point (z^*, t^*) in Fig. 5 is greater than the time interval, i.e. $t_1(z^*) < t^* - \Delta t$. This case arises for some points when the slices travel less than the slice spacing during the time interval. During operation, the distance simulated during each time interval increases with casting speed, but is usually less than the distance between slices. Specifically, the 75mm span in this work is achieved only for speeds of 4.5 m/min or more. At lower speeds, the points further along each jag in the casting direction are most accurate, because they contain the most recent temperature estimates.

7. Online Control System Development and testing:

A new dynamic control system, called “CONONLINE”, has been developed to control spray cooling in thin-slab casters, and has been implemented at the Nucor Steel casters in Decatur, Alabama. It is based on the control diagram in Fig. 7. The core of the system is a software sensor based on the CONID heat-conduction model. The software sensor, CONSENSOR, provides a real-time estimate/prediction of the strand state, including the shell surface temperature distribution and metallurgical length. It updates based on all the available casting conditions, which include: 1) conditions updated every second, such as mold heat flux, casting speed, spray flow rates, strand width, etc; 2) heat-specific conditions such as steel composition which are updated for heat changes during ladle exchanges; and 3) conditions updated only when the software sensor is calibrated, such as roll and spray nozzle configuration, heat transfer coefficients, etc.

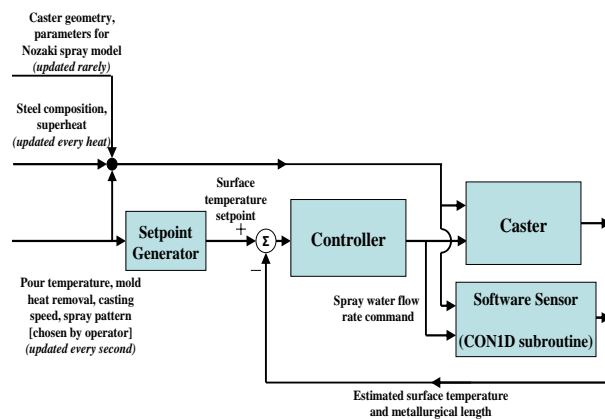


Fig. 7. Software sensor based control diagram

The estimated shell temperature profile is then compared against a pre-determined surface-temperature profile setpoint, which also varies with casting

conditions such as mold heat flux, as described later. The mismatch between the estimate and the setpoint, i.e. the tracking error, is then sent to a dynamic controller to compute the water flow rate command required to drive the mismatch to zero. Finally, the computed command set of spray-water flow rates is sent to the spray zone actuators in the operating caster (Level 1 control system), to the Monitor program for visual display to caster operator, and also to the software sensor for estimation at the next second.

This control system has been integrated with the Level 2 system of an operating thin-slab continuous caster, to control the spray water cooling flow rates in real time. CONCONTROLLER currently runs on a separate computer from CONONLINE, to ensure real-time output of spray commands even if the model runs slowly or crashes. The monitor runs on the model workstation, and takes advantage of GTK+ and GDK graphical user interface libraries. The two computers communicate with each other and the caster Level 2 system using network software and shared memory as shown in Fig. 8.

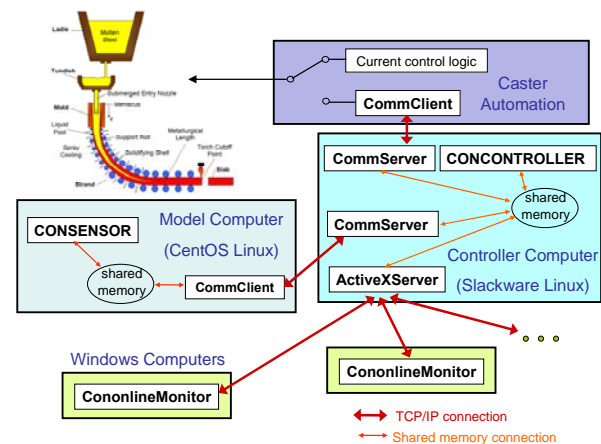


Fig. 8. Software sensor based control system architecture

7.1 Monitor. Fig. 9 shows a typical snapshot of the monitor. It was developed to provide clear and quick feedback to the plant operators and engineers. The data shown includes shell surface temperature, temperature setpoint, shell profile, metallurgical length, spray water flow commands, and casting conditions. This allows for monitoring of the control system performance, warning of dangerous operating conditions, and providing general information about the current state of the steel slab.

The importance of the monitor as part of the control system should not be underestimated. By presenting

accurate information to the operator in real time in a natural visual manner, this system empowers the operator to react better to unforeseen situations. In addition to controlling surface temperature, another important objective of the system is to avoid costly and dangerous “whale” formation. A whale forms when the metallurgical length extends past the last set of support rolls, and the internal ferrostatic pressure causes excessive bulging of the strand. While this system was being tested at Nucor Decatur on the North Caster, prior to giving it full automatic control, operators watching the monitor were able to recognize impending problems and avoided whale formation. The South Caster, which did not have the system, experienced a whale during this time.

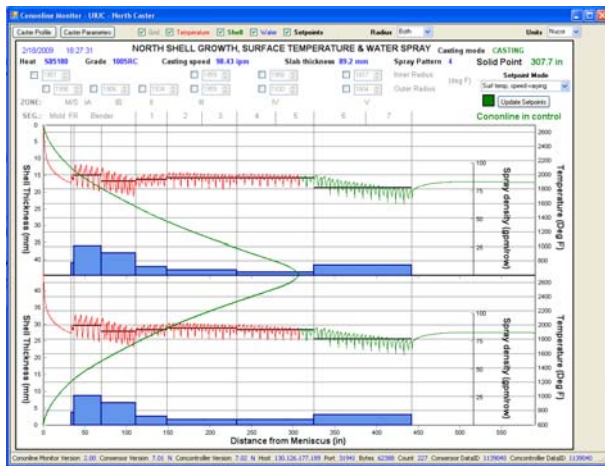


Fig. 9. Monitor interface displaying on both sides: the shell surface temperature profile, its corresponding setpoints, spray-water flow rates commanded and their setpoints, shell thickness profile prediction, and other information.

7.2 Controller Implementation. The accuracy of control is limited first by the actual casting equipment. A continuous caster is divided into spray zones, each zone having a single water flow input. This water flow rate is the actuator controlled by CONCONTROLLER. Although there is usually more than one spray zone across the width of the caster, the output of the software sensor is only for the centerline of the slab. The spray zones outside of the center of the caster require additional logic. Currently, they are fixed fractions of the central zone simulated by the model.

Fig. 10 shows the center spray zones of the caster at the Nucor Decatur steel mill. In the first four spray zones, inner and outer radius sprays are linked. In the remaining three zones, the inner and outer radius sprays may be separately assigned. Thus, a total of 10 independent spray commands are available.

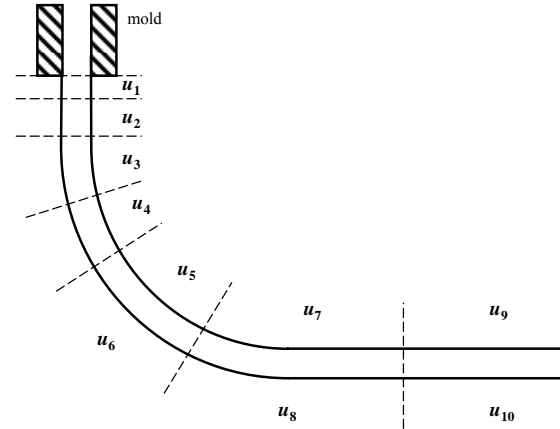


Fig. 10. Center spray area configuration

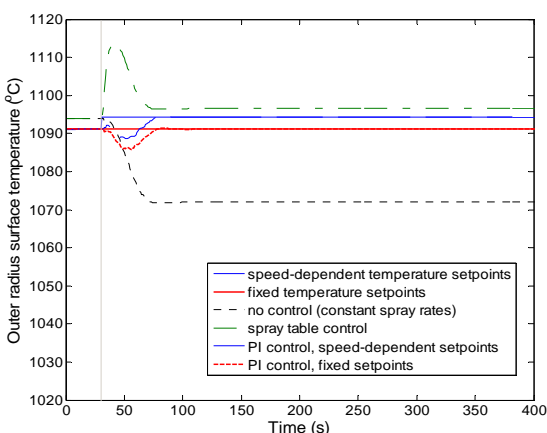
Because heat transfer between slices is negligible, the control of each spray zone may be governed by an independent control algorithm. Currently, these are single-input-single-output controllers. The possibility of using multiple-input-single-output or distributed-input controllers is a topic of continuing research.

Each controller follows the same general control algorithm. At each time step, the error between the shell surface temperature profile estimated by the software sensor and a setpoint temperature profile is averaged over the portion of the slab governed by the controller. This average temperature error is used to calculate control effort based on a proportional-integral control law. The gains are tuned separately for each spray command.

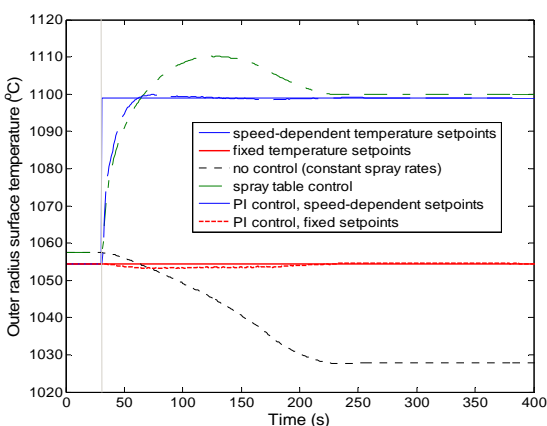
The actual spray command is limited to a range between turning closing the control valves and opening them completely, and so the effect of actuator saturation is a concern. Integrator windup can lead to over or undershooting should saturation occur during transient behavior. A classical anti-windup scheme [25] is applied to prevent integrator windup if the control command becomes negative or greater than the maximum possible spray rate. More detail on the controller design is given elsewhere.^[3, 11]

Choosing temperature setpoints is a challenging task that is on-going. Initial setpoints have been based on sets of water flow-rate setpoints that yield good performance in the steady state from past experience. A complete set of spray rates for all spray zones at all casting speeds is called a spray pattern. Each spray pattern is typically tuned for a specific grade of steel. It is designed to achieve a surface temperature history that avoids cracks, while solidifying the steel prior to exit from the containment region.

7.3 Control System Evaluation Study. Figs. 11 and 12 show results of offline testing using the control system. These figures show the outputs of the software sensor under different control strategies in order to illustrate some of the issues involved in implementing software sensor-based control. Running in real time, they include the same numerical errors encountered in the caster. In partnership with Nucor Steel Decatur, the model has been tested on an actual caster in “shadow mode”, and is currently being trialled for actual control of the process.



a) zone 2 (outer radius)



b) zone 8

Fig. 11. Zone-average temperatures during a sudden slowdown from 3.0 to 2.5 m/min casting speed, comparing four control methodologies.

Fig. 11 compares the performance of the online control system to the current spray practices during a sudden drop in casting speed from 3 to 2.5 m/min at 30s, with an accompanying drop in mold heat flux from 2.373 to

2.178 MW/m². The average outer-radius shell surface temperature in zones 2 and 8 (cf. Fig. 10) are plotted. The responses of several different control methodologies are compared, to illustrate the issues involved.

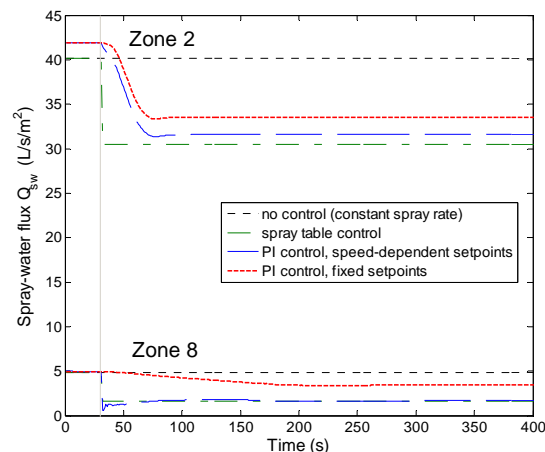


Fig. 12. Spray-water flow rates corresponding to Fig.11 example during a sudden slowdown from 3.0 to 2.5 m/min casting speed, comparing 4 control methodologies.

With no controller, spray-water flow rates remain constant with time, so the decrease in casting speed causes higher heat extraction at any given distance down the caster, and the surface temperatures all eventually drop. The time delay for the transition to the new lower steady-state temperature varies with distance down the caster. Steady state is not reached until steel starting at the meniscus at the transition time ($t = 30s$) finally reaches the given point in the caster, after being cast entirely under the new conditions. Thus, points nearer to the meniscus react quickly to the change, while points lower in the caster are affected by the changing upstream temperature history for a long time. In the figures, it is clear that zone 2 reaches steady state sooner than zone 8.

The current (old controller) spray practice is based on “spray-table control.” The spray flow rates in each zone down the caster, or “spray pattern” that produces good quality steel for a specific group of steel grades in a specific caster are determined from plant trial and error and previous experience. Higher casting speed requires higher water flow rates to maintain the same cooling conditions. Thus, for each spray pattern, a different spray profile is tabulated for each casting speed in a grid (database) that spans the range of normal operation. During casting, spray setpoints are interpolated from the appropriate spray-table database for the chosen pattern,

according to the current casting speed. This method has the disadvantage that it does not accommodate transient behavior in the strand.

With a controller that increases spray water in proportion to casting speed, the responses in **Fig. 11** show a characteristic temperature overshoot before settling to steady state. During a sudden speed drop, the spray rates drop immediately, as seen in **Fig. 12**. However, with the recently higher casting speed, the upstream steel is hotter than expected, so the surface temperatures overshoot the desired values at steady state. The steady-state temperatures at 2.5 m/min are larger than the steady-state temperatures at 3.0 m/min because the spray rates assigned at the lower speed are predicted by the model to be even lower than the drop in speed requires.

Previous metallurgical knowledge on optimizing spray cooling is defined in terms of steady-state surface-temperature profiles to avoid various embrittlement and cracking problems that are associated with particular temperature ranges.^[26] Furthermore, surface temperature variations with time, such as occur during speed changes, startup, and tailout, are detrimental because they cause surface stress and defects. To combine these two types of knowledge, the spray tables were converted to tables of surface temperature profile setpoints. This is a two-step process comprised of the generation of setpoint profiles offline, and the interpolation of these profiles during casting. To generate the setpoints, CON1D was run for every casting speed and all patterns according to the tabulated spray profiles. The resulting temperatures are stored in a two-dimensional array (according to speed and pattern). During operation, these profiles are interpolated to find the desired temperature profile for the current casting speed and pattern to use as the setpoint for the PI controller. This second approach is referred to as “speed-dependent temperature setpoints”.

With PI control using speed-dependent temperature setpoints, the overshoot is drastically reduced. In fact, in **Fig. 11a**, it can be seen that there is initially a slight undershoot in zone 2. As **Fig. 12** makes clear, this is because the spray flow rate command from the PI controller changes more gradually than spray-table control. However, the command changes as sharply as spray-table control in zone 8. This response is needed to achieve the larger change in temperature setpoints at the speed change. The later small decrease before finally reaching steady state is needed to avoid the overshoot.

However, the temperature setpoints need not vary with casting speed during operation. If the computational

model is reliable, it is better to use a constant temperature setpoint for all casting speeds. In this work, a representative profile was chosen from each pattern in the speed-dependent temperature-setpoint database, reducing the setpoint table by one dimension. This approach takes advantage of the fact that steel thermal properties are relatively independent of steel grade and casting speed, so that quality depends mainly on surface temperature profile.

During offline (shadow mode) plant testing, the controller output using fixed temperature setpoints called for many sharp changes in spray rate in the first few spray zones. It was discovered that this was caused by significant variations in strand surface temperature at mold exit with changes in mold heat flux, casting speed, and steel grade. Forcing the surface temperature to change quickly to a specified temperature setpoint causes detrimental sharp changes in shell surface temperature, especially in the first two spray zones below the mold. Such changes, and the associated thermal stresses, are what setpoint-based control is supposed to avoid.

The root of the problem is that temperature profiles are sensitive to the mold heat flux, which is not accounted for in the spray table. To generate the setpoints, the average mold heat flux, \bar{q}_{mold} , was estimated as, \bar{q}_{mold0} , by a function of mold powder and casting speed, from the empirical correlation in ^[12]. Even though this equation reasonably predicts mold heat flux at the caster in this work, (and could be tuned to be even better), the effects of unaccounted variables (such as mold powder changes, superheat effects, and random variations) always cause the measured mold heat flux, and the corresponding surface temperature at mold exit to change significantly with time at a given casting speed (setpoint).

To avoid this problem, a new setpoint strategy, called “fixed temperature setpoints” was developed that allows the temperature profile setpoints to vary with mold heat flux, and consequently with mold exit temperature. Five different temperature profile setpoint curves are generated using CON1D with $0.7 \bar{q}_{mold0}$, $0.85 \bar{q}_{mold0}$, \bar{q}_{mold0} , $1.15 \bar{q}_{mold0}$, and $1.3 \bar{q}_{mold0}$. An example of the 5 temperature setpoint curves for one particular pattern is shown in **Fig. 13**. It can be seen that these setpoints produce mold exit temperatures that span a wide range from 850 to 1250 °C. This third strategy again stores a two-dimensional array of fixed temperature setpoints (organized according to mold heat flux and pattern). During operation, these setpoints can be linearly interpolated against mold exit temperature to choose a temperature setpoint profile that includes a match with

the current mold exit temperature. The effect of mold heat flux variations diminishes with distance down the strand, so the setpoint is allowed to vary with mold exit temperature only in the first four zones. The temperature setpoint for the remaining zones uses the original fixed setpoint corresponding with \bar{q}_{mold0} . The impact of mold heat flux variations is thus evenly distributed over the first 4 spray zones and thereby avoids sharp spray rate changes and corresponding surface temperature changes in the first few spray zones.

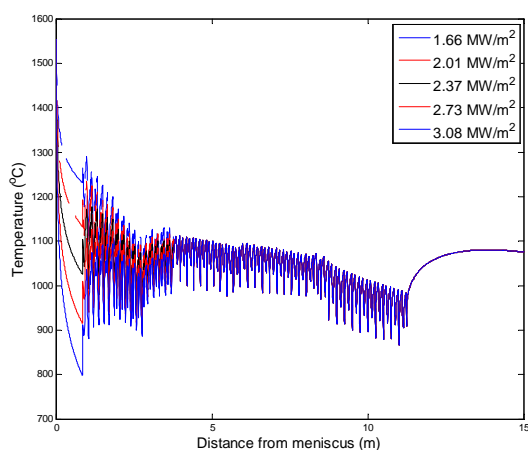


Fig. 13. The 5 temperature setpoint curves for spray pattern 4 with varying mold heat removal rates.

Finally, these results illustrate the superiority of PI control using fixed temperature setpoints. With this controller, the surface temperature is kept remarkably constant through the speed change. To achieve this, **Fig. 12** clearly shows how the sprays are gradually decreased after the speed change, and the further the zone is from meniscus, the more gradually the spray rate is changed. The steady-state spray-water flow rates are properly smaller at the lower casting speed.

This case study demonstrates that all of the controllers perform as expected. The PI controller with fixed setpoints produces the best response for steel quality, as detrimental surface temperature fluctuations are lessened. Temperature estimate in the mold is quite accurate, because it is based on the measured mold heat removal rate. Because strand surface temperature cannot be measured accurately and robustly in real time, surface temperature estimate accuracy could deteriorate with distance below mold exit. Thus, CONSENSOR is strictly termed an *open loop observer* of the strand temperature profile, with its estimate in the secondary cooling region accurately initialized at mold exit. To improve the system thus requires lab measurements of

heat transfer coefficients during air-mist spray cooling and further calibration with plant measurements.

This new software-sensor based control system will improve steel quality at the steel plant, by maintaining temperature in the process more closely during transients. An advantage of CONONLINE, beyond its use for control, is that it offers more information to plant engineers and operators regarding the effect that casting conditions have on the strand. Moreover, the system, which runs in real time and accurately represents the behavior of a real caster, is a valuable research tool that enables scientific investigation of the continuous casting process. Future advances in control strategies and quality understanding can now be investigated using this system.

8. Laboratory measurement of water flow and heat transfer during spray cooling: Experiments have been initiated as part of this project to gain a more fundamental understanding of water spray cooling at high temperatures.^[12] The experiments are being conducted in Saltillo, Mexico in co-operation with Cinvestav, a national research organization, owing to availability of specialized laboratory facilities for this type of research, and previous successful work in this field by Drs. Castillejos and Acosta.^[27]

The research in this project aims to measure heat transfer in the secondary spray cooling zones of steel continuous casting machine to characterize the boundary conditions at the strand surface for CONONLINE (Eq. 2). Work here focuses on water jet / air mist or “pneumatic” cooling in the surface temperature range of 1300-700°C. The effects of different air and water pressures, water impact density, time scales of the transient phenomena at the hot surface, water composition, and surface roughness are being investigated.

Historically, hydraulic nozzles that only use water for cooling are used. Lately, pneumatic nozzles which force water out of the nozzle with pressurized air are becoming more popular because cooling is more uniform and has higher efficiency. Cooling from these “air-mist” nozzles depends on the characteristics of spray, e.g. droplet size and velocity, and is not well understood. Heat transfer is controlled by complex mechanisms involving dynamic buildup of steam layers, film boiling, droplet impacting through these layers, and Leidenfrost effects. Careful experiments and analysis are needed to improve fundamental understanding and characterize this behavior, in order to accurately predict heat transfer.

8.1 Water Flow Experiments. The first step to understand how heat transfer occurs is to measure the impact density, i.e. amount of water impacting in a unit area in unit time. The spray water exiting the nozzle is measured for a specific time using an unheated plate perforated with holes connected to tubes, called a “water collector”. Impact density is calculated knowing the size of each collector hole and the spraying time. This is repeated for maximum and minimum operating conditions to see the changes caused by changes in water and air pressures. In Fig. 14, typical results are shown for a nozzle at both maximum and minimum operating conditions.

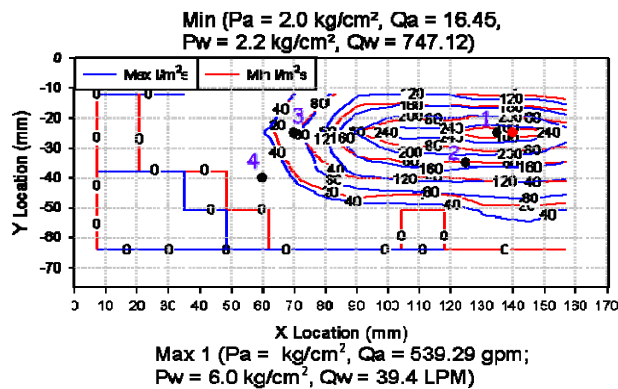


Fig. 14. Spray pattern corresponding to minimum and maximum operating conditions. Black dots thermocouple locations and the red dot is the nozzle centerline.

In this project, the spray patterns of all the Delavan Spray Technology nozzles used in the Nucor Decatur and Riverdale casters were measured. The water spray rate maps give the shape of the water droplet impact distribution over the height of the pattern and are needed for developing a fundamental-based model of heat transfer convection rates. This measurement also provides a simple method to maintain uniform heat transfer by showing how to position nozzles to cover the whole area it is designed to cool.

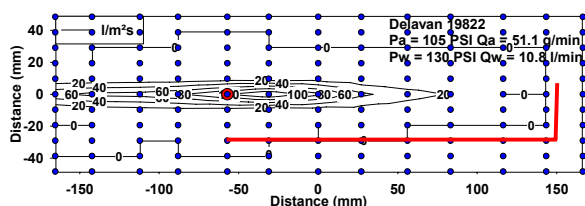


Fig. 15. Measured spray pattern and corresponding width from the caster blueprints marked a red line. Blue dots collector locations and the red dot is the nozzle centerline.

During this research, it was found that two of the nozzles were not, in fact, covering the whole width of the area that they were supposed to cool as shown in Fig. 15. Changes have been made in the caster to correct the overheating problems that occur in between nozzles in these places. Results for all of the nozzles are presented elsewhere.^[14]

8.2 Transient Cooling Experiments. Next, the apparatus shown in Fig. 16 is used to measure heat transfer under transient cooling conditions. A sample steel plate is instrumented with thermocouples at appropriate locations (based on the water collector results), it is heated up to between 700 and 1300°C, transported quickly to the spray station, and quenched down to room temperature using different air and water pressures. Typical measured cooling curves are shown in Fig. 17.

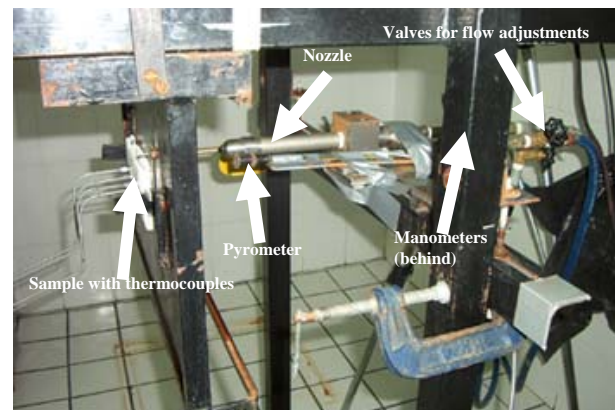


Fig. 16. Unsteady state measurement apparatus.

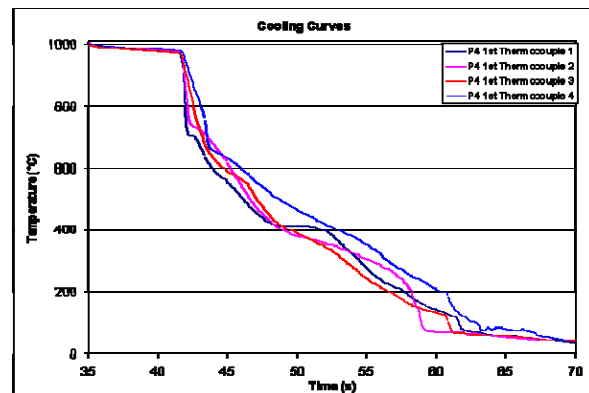


Fig. 17. Cooling curves from a transient experiment

Heat flux and temperature on the surface of a sample is determined using a computer program CONTA developed in Michigan State University and Sandia National Laboratories. The program solves nonlinear, one-dimensional planar inverse heat conduction

problem (IHCP) using finite difference method (FDM) based on implicit Crank-Nicolson method. When measuring large cooling rates, the calculated heat flux has errors, as they do not reproduce the measured temperatures when used as the boundary condition of a direct heat transfer solver. To overcome this problem, the original data was augmented by linear interpolating new data between the measured data points. An example set of results showing the improved curve is given in **Fig. 18**. Complete results for all of the different nozzles are presented elsewhere.^[13]

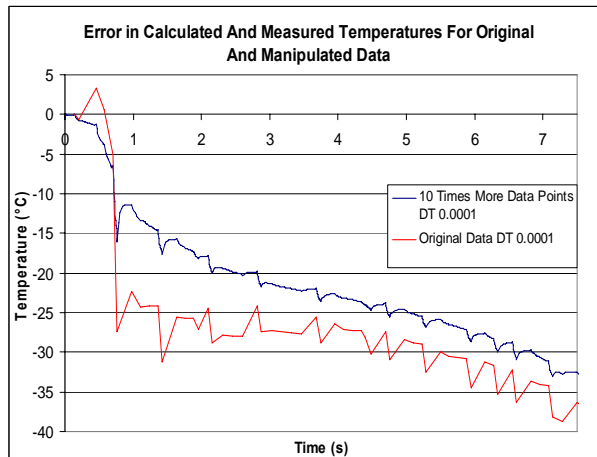


Fig. 18. Heat flux values from centre of a water spray nozzle impact pattern as a function calculated surface temperature.

8.3 Steady-State Heat Flow Measurements. With the high cooling rates of air-mist nozzles, the temperature drops very quickly during the transient experiment, so heat transfer coefficients correspond with only a few seconds of data. However, forming a stable steam layer may take more time, especially with the small droplets of air-mist cooling. Thus, spray heat transfer is likely dynamic and is a complex function of droplet momentum, surface roughness, and surface temperature.

To overcome this problem, this work is adopting another approach to investigate spray cooling by maintaining the sample at a constant temperature while spraying it. An apparatus was designed and constructed for this purpose, shown in **Fig. 19**.

To minimize oxidization, platinum is used as the sample material instead of steel for the initial experiments. To maintain constant temperature, the sample is heated by induction coils while it is sprayed. Induction current is controlled to maintain the temperature monitored by a thermocouple via closed-loop control. During each experiment, the sample is heated in stages from 100 °C

to 1300 °C in steps of 100 °C, as shown in **Fig. 20**. At each step, sample temperature is held for 7 minutes, while temperatures in the sample and ceramic body and the power input are all recorded (**Fig. 20**). This method enables measurement of the transient heat extraction changes that occur during spraying at a constant temperature independently from the changes due to changing temperature.

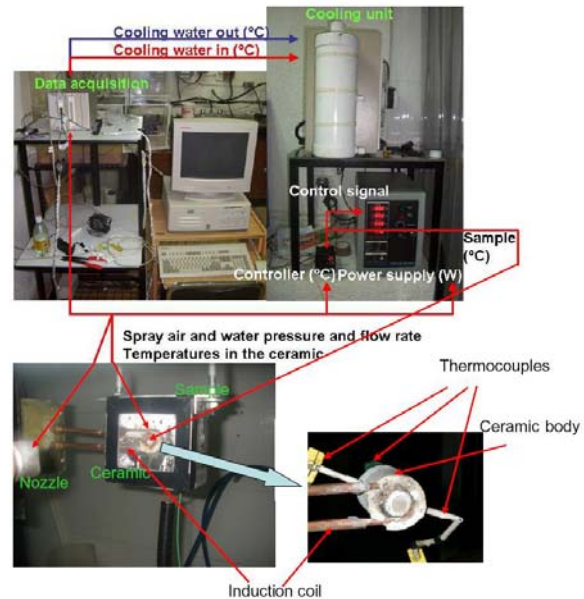


Fig. 19. New steady-state measurement apparatus

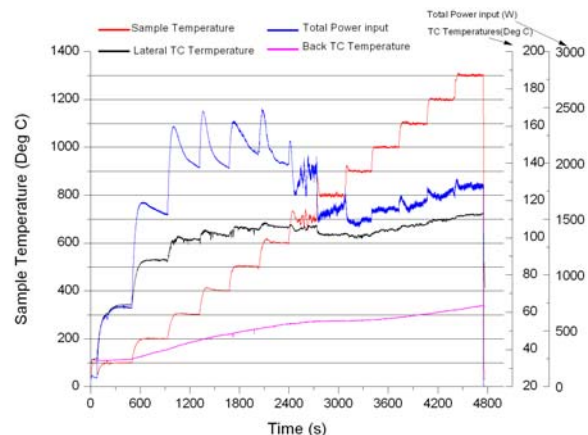


Fig. 20. Sample heating up path with lateral thermocouple temperature, back thermocouple temperature and total input power.

To interpret the experimental measurements (ie. extract the spray heat transfer coefficients), a two-dimensional axisymmetric transient heat-conduction model has been constructed using the commercial FEM-based software package COMSOL (www.comsol.com). The domain,

shown in **Fig. 21** includes the sample, the copper coil, and the ceramic body. Each simulation begins by solving for the quasi-static vector magnetic potential field and the resulting heat generation from both the induced and applied currents is input as a source term to the heat transfer calculation. Since the copper induction coil consists of 1.5 loops, both 2-D axisymmetric geometries are created of both both 1-loop and 2-loop geometries and the final predictions are generated by combining results appropriately from simulations of both geometries.

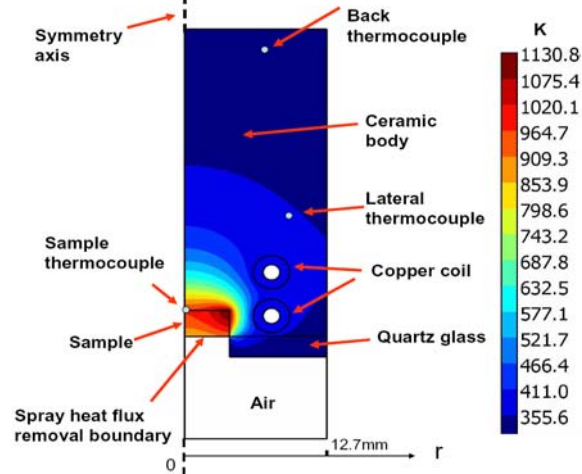


Fig. 21. Model domain for 2-loop geometry with temperature contours (600°C sample temperature).

Spray heat transfer predictions based on this steady-state model together with results from transient measurements are shown in **Fig. 22**.

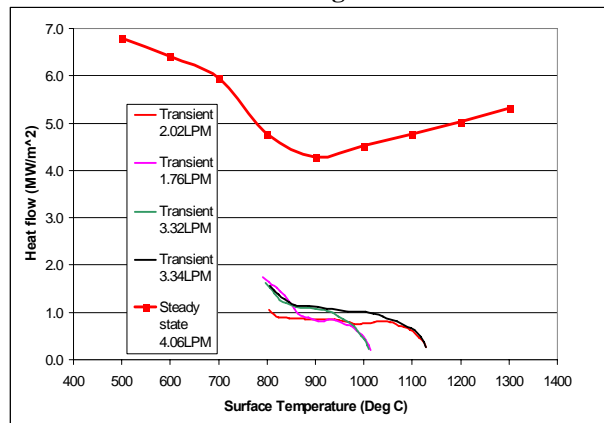


Fig. 22. Heat flux at centre of a water spray nozzle impact pattern as a function calculated surface temperature.

The preliminary results in **Fig. 22** suggest that heat transfer coefficients of the steady-state experiment are

much higher than the transient experiment. This might be due to the time needed to establish the boundary layer of steam, thermocouple delays in transient experiments, or inaccuracy of COMSOL 2-D models simulation on steady state experiments. The heat flow for steady state experiments decreases from 500°C to 900°C and above that increases. This behaviour is similar to that expected for the transition from transition boiling (Leidenfrost effect) to stable film boiling. Much further work is needed to confirm these initial results with replicate experiments, with the help of improved measurement of power, external current measurement, cooling water temperature measurements, more efficient copper coil design, and better insulation of the sample and ceramic body from moisture and heat losses, for different spray cooling conditions. Finally, a 3-D heat transfer model is being constructed to validate the 2-D model, and to match simultaneously with all of the measurements. More details on this work are given elsewhere.^[12]

9. Steel Plant Experiments for Model Validation and Calibration: Experimental trials have been carried out at Nucor Steel, Decatur, Alabama, and at Mittal Steel, Riverdale, in order to measure slab surface temperature variations with optical pyrometers. In addition, mold heat flux is measured from the temperature rise of the cooling water, knowing the water flow rate. These results are being used to calibrate the CONID model. Results for both casters were presented previously.^[7, 17]

Experimental trials were carried out at Nucor Steel, Decatur, Alabama on Jan 12-17, 2006, to measure the variation of slab surface temperature under different casting conditions, varying the casting speed and spray water flow rates. These results were used to calibrate the CONID model. Mold heat flux is measured from the temperature rise of the cooling water, knowing the water flow rate. To measure surface temperature, two-color optical pyrometers were installed at four different locations in the spray zones. The four Modline® 5, 5R-141000, 4M5#25579 pyrometers were positioned at 3861, 6015, 8500 and 11384 mm below the meniscus.

Initial casting experiments included three different trials: i) Changing spray pattern at constant casting speed change at north caster (01/13/06 9.52 am – 10.04 am (shown in part in **Fig. 23**, south caster 01/13/06 16.12 – 16.37); ii) changing casting speed with spray water flow pattern design at south caster 01/16/06 10.10 am – 10.57 am; iii) changing casting speed at spray water flow pattern design (sprays constant except for foot roll and upper bender segments that were left dependent on casting speed) at south caster 01/16/06

20.20 – 21.04. Typical steel grade was 0.247%C and pour temperature

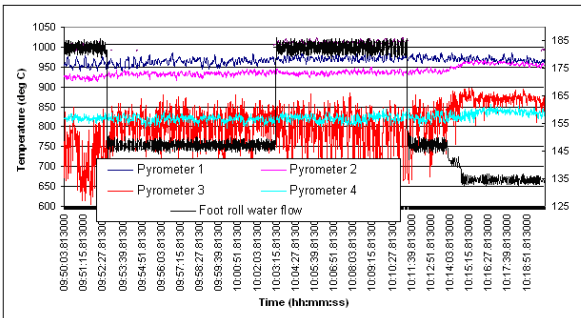


Fig. 23. Pyrometer Data during spray water change trial 1 (3.5 m/min; spray pattern 4)

The data from the caster Level II system was recored as *.dat files for analysis in ibaAnalyzer 4.3.3 and *.xls.

The pyrometer measurements varied throughout the experiments, due to the intermittent presence of steam, and possibly also due to variations in emissivity of the surface scale layer. For the sample raw data given in **Fig. 23**, (trial 1), pyrometers 1, 2 and 4 are seen to have relatively uniform temperatures while pyrometer 3 fluctuates over several hundred degrees. Blowing the steam away with a fan was found to increase and stabilize the pyrometer temperatures, producing the mean values included as part of **Fig. 24**.

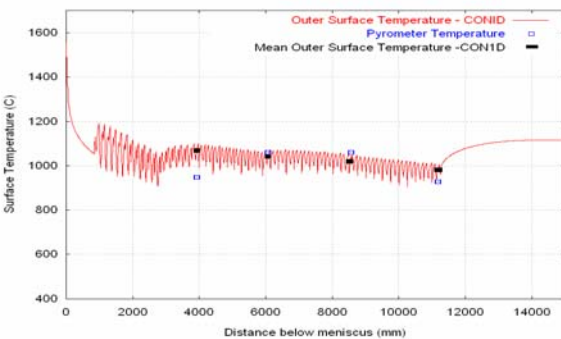


Fig. 24. Surface temperature history at steady state, comparing CONID model predictions and steel plant measurements (3.5 m/min; spray pattern 4)

To compare with the pyrometer measurements, the varying surface temperatures computed by the CONID model are averaged over 20mm of strand surface within the varying jet impingement region, which corresponds to the region that the pyrometer measures (in between rolls). This mean temperature is compared with the 4 pyrometer measurements in **Fig. 24**, along with the entire temperature profile. The agreement is reasonable,

although further calibration is needed. **Fig. 24** also reveals the variations in the surface temperature, which need further work to validate. The results from this run show that the entire processing time for this 90-mm thick strand from liquid to complete solidification takes only 1-3 minutes. Casting speed variations from 3-5m/min result in metallurgical lengths ranging from 6-13m for these typical thin slab casters. The metallurgical length for the 3.5m/min case shown is ~11m.

Although model validation is ongoing, the CONID model is judged to be sufficiently accurate to implement into the control model.

At Mittal Riverdale, surface temperature is measured for different casting speed and spray water flow rates using four pyrometers: including one at the bend, (10256mm below the meniscus), one at the shear, (14550mm below meniscus), and two in the spray zones. So far, three trials (trial 1 on Sep.11th, trial 2 on Oct.19th and trial 3 on Mar.12th) have been conducted at steady conditions. Simulations of six cases (case 1~6, two for each trial) have been performed to predict the strand surface temperature, which are then compared with the pyrometer measurements.

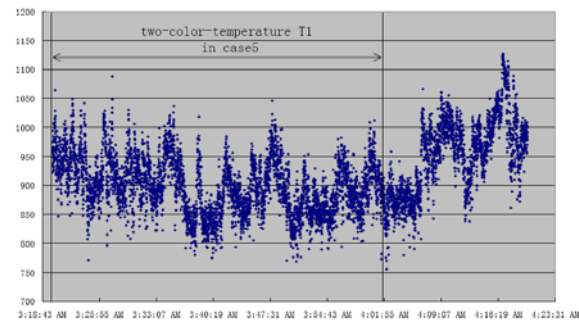


Fig. 25. Two-color-temperature T1 in case 5

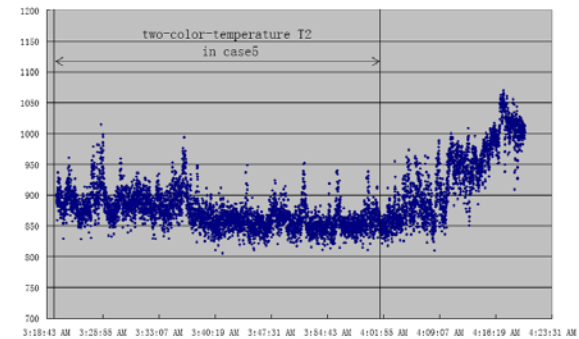


Fig. 26. Two-color-temperature T2 in case 5

The pyrometer measurements fluctuated throughout the trials, due to the intermittent presence of steam, possible

variations in emissivity of the surface scale layer, and changes in casting conditions. Time periods of steady casting, with relatively uniform pyrometer temperatures, were chosen to get average measured temperatures.

Fig. 25 and **Fig. 26** show typical spray-zone pyrometer measurements for case 5 in trial 3. These pyrometers were put in the same location of segment 2, 5361mm below meniscus. Pyrometer measurements varied by 20°C between different two-color methods and 200°C over 90 minutes time intervals of roughly steady casting. The ~40-minute time period over which the measured temperature is averaged, is also shown in the figures.

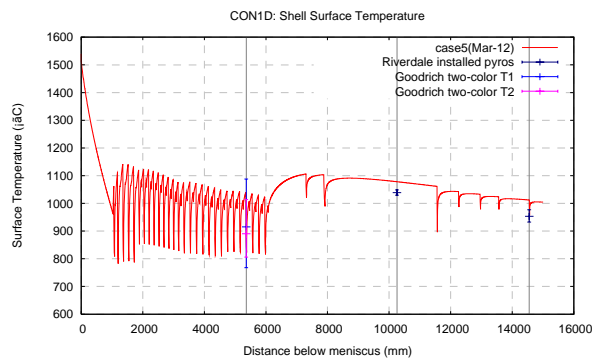


Fig. 27. Temperature prediction and comparison

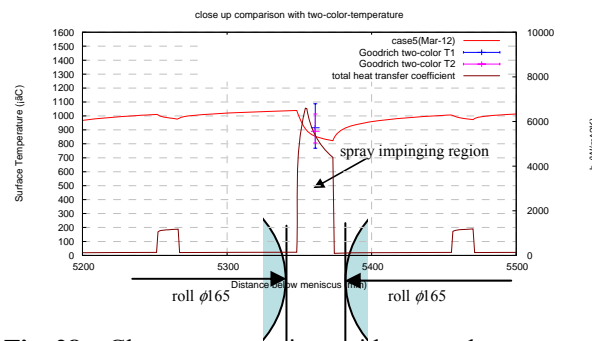


Fig. 28. Close up comparison with two-color temperature

Fig. 27 and **Fig. 28** show simulation results for case 5. Measurements from the pyrometers are included for comparison. The model temperature predictions are mainly within the scatter of the measurements, so are considered to be reasonable. This degree of agreement was also found for most casting conditions in other cases, especially within the spray zones.

The results from this run show that the entire processing time for this 55-mm thick strand from liquid to complete solidification takes only 1-2 minutes. A casting speed of 4.5m/min results in a metallurgical length of 4.6m for this typical thin slab caster.

Validation and improvement of the CON1D model is still ongoing. In the meantime, the model has been implemented into the CONONLINE control model system and is being tested in the plant, where quantitative accuracy is not essential to improve over the existing control model.

10. Understanding Defect formation during Continuous Casting:

To gain maximum benefit from a new spray-water control system, it is important to have a fundamental understanding of how defects form in the process. Parallel research is ongoing to achieve this aim. Work has been initiated to gain new insight into the mechanism of formation of defects associated with secondary spray cooling. These surface defects often initiate in the mold,^[28] especially at the meniscus,^[29] and later form surface cracks far below the mold in the secondary spray cooling zones.^[26] Cracks form at the roots of oscillation marks, which are prone to transverse crack formation during the spray cooling, depending on the temperature history. Thus, oscillation mark depth is also being studied. To avoid cracks, it is often necessary to keep the strand above a certain critical temperature, such as the Ar_3 temperature, $\sim 700^\circ\text{C}$. A comprehensive model of supersaturation, nucleation, precipitate formation, and grain size prediction is being developed to predict the dynamic evolution of the precipitate size distribution, including kinetic effects due to diffusion delay. This predictive tool is important to the optimization of temperature setpoint profiles to avoid stress (such as occurs during bending and unbending) when the surface is embrittled in a temperature range that is susceptible to transverse cracks. This work will be reported elsewhere.^[18]

11. Control of Mold Fluid Flow:

Many casting defects are caused by problems with fluid flow in the mold. To control fluid flow in the mold, an electromagnetic brake (EMBr) force is applied in many thin slab casters, including Nucor. A computational fluid flow model has been developed and applied to investigate the effects of varying SEN submergence depth and EMBr field strength on flow in the mold cavity.^[16] The three-dimensional, steady $k-\epsilon$ model of the nozzle and liquid cavity in the mold used the magnetic induction method in FLUENT to incorporate the localized-type static EMBr field measured at a steel plant. The model was validated by comparing results with an analytical solution and with nail board and oscillation mark measurements collected at the plant (see **Fig. 29**). Increasing EMBr strength at a constant SEN depth is found to cause a deeper jet impingement, weaker upper recirculation zone and meniscus velocity, and a smaller meniscus wave. Increasing SEN depth without EMBr caused the same trends. Increasing SEN

depth at a constant EMB strength brought about the opposite: higher meniscus velocity, larger meniscus wave, and deeper penetration depth. Using the knowledge gained from this model, electromagnetic forces can be controlled to stabilize the fluid flow in the mold cavity and thereby minimize casting defects.

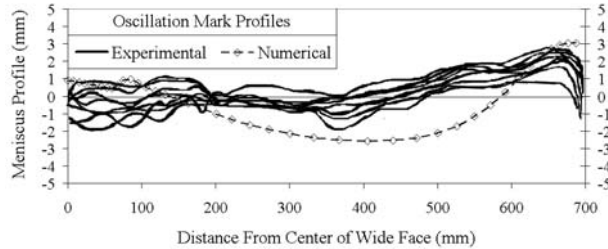


Fig. 29. Comparison of calculated meniscus profile from Case 6 with oscillation marks

12. Advanced Control Algorithm Development:

Rejection of broad classes of disturbances in systems with unknown parameters, but known parameter structure is a nontrivial practically important problem. In the finite-dimensional case, this problem is typically addressed through adaptive control laws modified to reject the disturbance class of interest. However, the standard finite-dimensional adaptive control configurations, such as those falling under MRAC, do not, in general, transition into the infinite-dimensional setting in a well-posed manner. Therefore, attaining similar disturbance rejection performance in distributed parameter case presents a considerable challenge.

This setting is of interest in a solidifying shell temperature control in continuous steel casting, where a single two-dimensional boundary control problem of the outer shell surface temperature shown in **Fig. 30** can be well approximated by a pair of one-dimensional distributed control problems of the outer shell surface temperature for the inner and the outer caster radii. This is accomplished by bringing in, as shown in the **Fig. 30** low, the near-constant distributed disturbance.

The latter is characterized by an approximately known model and represents the heat flux at the interface between the inner surface of the solidifying shell and the liquid core. The disturbance is seen to lie in the system input space. Thinking along the lines of this approximation governs, to a large extent, current spray cooling control practice at some key steel casting facilities.

In this application, actuation is designed to be a very close approximation of the distributed one to ensure smooth cooling along the strand - the feature especially important in continuous thin slab metal casting due to the thinness of the solidifying shell, and a matching

pyrometer array temperature sensing is being currently developed. The parameters of the casting process, such as heat transfer coefficients, are known to be periodic-like functions of a spatial variable due to the fact that the outer shell surface alternates between being in contact with the fixed position support rollers and being subject to the water flux from the sprays along the cooling zone of a caster. This functional dependence is known, however, only approximately, is influenced by a number of factors, such as steel grade and casting speed, and undergoes a slow time-variation caused by the solidifying shell motion. Reduction of uncertainty in this dependence is currently underway; however it proves to be very costly, time consuming, and requiring nontrivial instrumentation. In addition, the pyrometer readings are characterized by a noticeable steam-induced spatiotemporal noise.

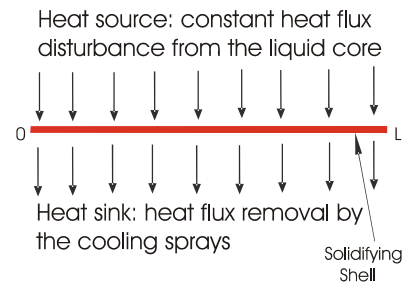


Fig. 30. Approximation of the single 2D shell surface temperature boundary control problem by the two - outer and inner radii - 1D shell surface temperature distributed control problems through the introduction of the constant distributed heat flux disturbance. The latter is induced at the liquid/solid interface by the molten steel core encased by the solidifying shell

This problem is solved in ^[6]. Based on the well-posed MRAC configurations recently introduced ^[4] that are free from plant output spatial derivatives, this work develops the well-posed error systems and the corresponding robust MRAC laws with disturbance rejection for a class of systems represented by parabolic or hyperbolic PDEs with spatially varying parameters. Disturbances are assumed to be generated by a known model and lie in the system input space. Control signal is, then, shown to include the disturbance estimate generated by the corresponding distributed parameter Luenberger-type observer. The well-posed error systems and the corresponding algorithms for parabolic and hyperbolic PDEs are derived, with the disturbance rejection properties exhibited in numerical simulations. For simplicity, derivations are carried out for a single spatial domain. The paper considers distributed sensing and actuation as well as distributed disturbance.

Plant: $u_t = (a(x)u_x)_x + b(x)u + f(x,t) + d(x,t)$

Reference Model: $v_t = (a_1(x)v_x)_x + b_1(x)v + r(x,t)$

Adaptive control law: $f = r + \varepsilon_0 e + \eta_{a1} v_{xx} + \eta_{a2} v_x + \eta_b v$

Disturbance model: $d_t = (a_d(x)d_x)_x + f_d$

Schematic of adaptive controller and disturbance observer is given by **Fig. 31**.

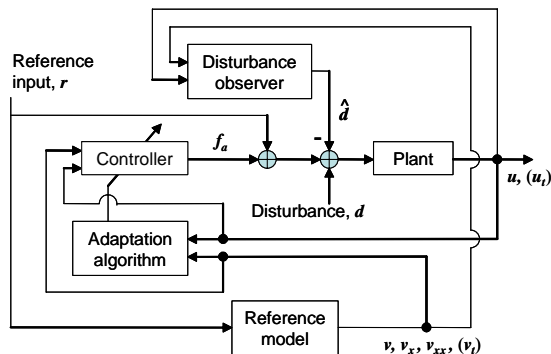


Fig. 31. Adaptive controller and disturbance observer

13. Conclusions: A new software-sensor-based system to control temperature in the spray-cooling zones of continuous steel thin-slab casters has been created, tested, validated with lab and plant measurements, and successfully implemented into a commercial steel plant. This report has summarized the results of seven different sub-projects which comprise this multi-faceted research project. Further details can be found in 16 publications,^[3-18] a pending patent,^[19] and in the website <http://ccc.mechse.uiuc.edu>.

14. Acknowledgments: This work is supported by the National Science Foundation (Grant # DMI-0500453) and the Continuous Casting Consortium at the University of Illinois. Thanks are also extended to industry collaborators at Nucor Steel, Decatur, AL, including Ron O'Malley; Delevan Spray Technologies, including Stephen Swoope and Mittal Riverdale, including Clint Graham. The authors also wish to thank the National Center for Supercomputing Applications at the University of Illinois for computing time.

15. References:

1. World Steel in Figures, 2006, International Iron Steel Institute, Brussels, Belgium, www.worldsteel.org.

2. J.K. Brimacombe, P.K. Agarwal, S. Hibbins, B. Prabhaker and L.A. Baptista: "Spray Cooling in Continuous Casting," in *Continuous Casting*, vol. 2, J. K. Brimacombe, ed., 1984, pp. 105-123.

3. Bryan Petrus, Kai Zheng, Brian G. Thomas and Joseph Bentsman: "Real-Time Model-Based Spray-Cooling Control System for Steel Continuous Casting," *Metals and Materials Transactions B*, 2009, pp. submitted March, 2009.

4. J. Kim and J. Bentsman: "Robust Model Reference Adaptive Control of Parabolic and Hyperbolic Systems with Spatially-varying Parameters," *Proc. 44th IEEE Conference on Decision and Control*, Seville, Spain, Dec. 13-15, 2005, 2005, pp. 1503-1508.

5. J. Kim and J. Bentsman: "Multiresolution Finite-Dimensionalization of Parameter Update Laws in Adaptive Control of Distributed Parameter Systems," *Proc. 45th IEEE Conference on Decision and Control*, San Diego, CA, Dec. 13-15, 2006, 2006, pp. 2801-2806.

6. J. Kim and J. Bentsman: "Disturbance Rejection in Robust Model Reference Adaptive Control of Parabolic and Hyperbolic Systems," *Proc. 45th IEEE Conference on Decision and Control*, San Diego, CA, Dec. 13-15, 2006, 2006, pp. 3083-3088.

7. B.G. Thomas, J. Bentsman, K. Zheng, S. Vapalahti, B. Petrus, A. Behera, A.H. Castillejos and F.A. Acosta: "Online Dynamic Control of Cooling in Continuous Casting of Thin Steel Slabs," in *Proceedings of 2006 NSF Design, Service, and Manufacturing Grantees and Research Conference*, W. DeVries and M. Leu, eds., St. Louis, Missouri, July 24-27, 2006, 2006, p. 11p.

8. J. Kim and J. Bentsman: "Disturbance Rejection in a Class of Adaptive Control Laws for Distributed Parameter Systems," *International Journal of Adaptive Control and Signal Processing*, 2009, vol. 23, pp. 166-192.

9. K. Zheng and J. Bentsman: "Input/Output Structure of the Infinite Horizon LQ Bumpless Transfer and Its Implications for Transfer Operator Synthesis," *International Journal of Robust and Nonlinear Control*, 2008, p. revision submitted.

10. K. Zheng and J. Bentsman: "Decentralized Compensation of Controller Uncertainty in the Steady-State Bumpless Transfer Under the State/Output Feedback," *International Journal of Robust and Nonlinear Control*, 2008, p. in press.

11. K. Zheng, B. Petrus, B.G. Thomas and J. Bentsman: "Design and Implementation of a Real-time Spray Cooling Control System for Continuous Casting of Thin Steel Slabs," in *AISTech 2007, Steelmaking Conference Proceedings, Indianapolis, May 7-10, 2007, 2007*.
12. S. Vapalahti, B. G. Thomas, S. Louhenkilpi, A.H. Castillejos, F. A. Acosta and C. A. Hernandez: "Heat Transfer Modelling of Continuous Casting: Numerical Considerations, Laboratory Measurements and Plant Validation," *Proc. STEELSIM 2007*, Graz, Austria, Sept. 12-14, 2007, 2007.
13. S. Vapalahti, H. Castillejos, Andrés Acosta, Alberto C. Hernández and B.G. Thomas, Spray Heat Transfer Research at CINVESTAV, 2007, University of Illinois, June 12, 2007, Continuous Casting Consortium Report CCC0704.
14. S. Vapalahti, H. Castillejos, Andrés Acosta, Alberto C. Hernández and B.G. Thomas, Delavan Nozzle Characterization Research at CINVESTAV, 2007, University of Illinois, June 12, 2007, Continuous Casting Consortium Report CCC0703.
15. K. Zheng, T. Başar and J. Bentsman: "H ∞ Bumpless Transfer under Controller Uncertainty," in *Proceeding of the 46th IEEE Conference on Decision and Control*, New Orleans, LA, Dec. 12-14, 2007, 2007, pp. 2129-2134.
16. K. Cukierski, and B.G. Thomas: "Flow Control with Local Electromagnetic Braking in Continuous Casting of Steel Slabs," *Metals and Materials Transactions B*, 2008, vol. 39B (1), pp. 94-107.
17. B.G. Thomas, J. Bentsman, B. Petrus, S. Vapalahti, H. Li, A.H. Castillejos and F.A. Acosta: "GOALI: Online Dynamic Control of Cooling in Continuous Casting of Thin Steel Slabs," in *Proceedings of 2008 NSF CMMI Engineering Research and Innovation Conference*, Knoxville, Tennessee, Jan. 7-10, 2008, 2008, p. 16p.
18. Kun Zhu and Brian G. Thomas: "Prediction of Grain Size, Precipitation, and Crack Susceptibility in Continuous Casting," *Proc. AISTech 2009 Steelmaking Conference Proc.*, St. Louis, MO, May 4-7, 2009, 2009, vol. 1.
19. Brian G. Thomas, Joseph Bentsman and Kai Zheng: "Spray Cooling Control System for Continuous Casting of Metal," United States, Patent Application No. 12/151/582, May 7, 2008.
20. Y. Meng and B.G. Thomas: "Heat Transfer and Solidification Model of Continuous Slab Casting: CON1D," *Metal. & Material Trans.*, 2003, vol. 34B (5), pp. 685-705.
21. T. Nozaki: "A Secondary Cooling Pattern for Preventing Surface Cracks of Continuous Casting Slab," *Trans. ISIJ*, 1978, vol. 18, pp. 330-338.
22. R.A. Hardin, H. Shen and C. Beckermann: "Heat Transfer Modeling of Continuous Steel Slab Caster Using Realistic Spray Patterns," *Proc. Modelling of Casting, Welding and Advanced Solidification Processes IX*, Aachen, Germany, 2000, pp. 729-736, 190.
23. B.G. Thomas and C. Ojeda: "Ideal Taper Prediction for Slab Casting," *Proc. ISSTech Steelmaking Conference*, Indianapolis, IN, USA, 2003, vol. 86, pp. 396-308.
24. Carlos Cicutti, MartinValdez, Teresa Perez, G. DiGresia, W. Balante and J. Petroni: *Steelmaking Conference Proceedings*, 2002, vol. 85 pp. 97-107.
25. C. Edwards and I. Postlethwaitex: "Anti-windup and Bumpless Transfer Schemes," *Proc. UKACC International Conference on CONTROL*, 1996, pp. 394-399.
26. M. M. Wolf: *Continuous Casting: Initial Solidification and Strand Surface Quality of Peritectic Steels*, vol. 9, Iron and Steel Society, Warrendale, PA, 1997, pp. 1-111.
27. Castillejos A. H. and F.A. Acosta: in *Proc. of 33rd McMasters Symp. on Iron & Steel Making*, 2005, pp. 47-58.
28. Y. Meng and B.G. Thomas: "Simulation of Microstructure and Behavior of Interfacial Mold Slag Layers in Continuous Casting of Steel," *ISIJ International*, 2006, vol. 46 (5), pp. 660-669.
29. J. Sengupta, B.G. Thomas, H.J. Shin, G.G. Lee and S.H. Kim: "Mechanism of Hook Formation during Continuous Casting of Ultra-low Carbon Steel Slabs," *Metallurgical and Materials Transactions A*, 2006, vol. 37A (5), pp. 1597-1611.